ARTICLE

Orientation and Structure of Ionic Liquid Cation at Air/[bmim][BF_4] Aqueous Solution Interface

Gang-hua Deng[a], Xia Li[b], You-qi Guo[c], Shi-lin Liu[a], Zhou Lu[b*], Yuan Guo[b*]

a. Hefei National Laboratory for Physical Sciences at the Microscale, University of Science and Technology of China, Hefei 230026, China
b. Beijing National Laboratory for Molecular Sciences, State Key Laboratory of Molecular Reaction Dynamics, Institute of Chemistry, Chinese Academy of Sciences, Beijing 100190, China
c. Nanjing University of Aeronautics and Astronautics, Nanjing 211106, China

(Dated: Received on May 14, 2013; Accepted on June 4, 2013)

The water-miscible room temperature ionic liquid 1-butyl-3-methylimidazolium tetrafluoroborate ([bmim][BF_4]) is a model system for studying the interactions between ionic liquid and water molecules. In this work the orientational structure of the low concentrated aqueous solution of [bmim][BF_4] at the air/liquid interface was investigated by sum frequency generation vibrational spectroscopy. It has been found that at very low concentrations, the butyl chain exhibited a significant gauche defect, indicating a disordered conformation; and the cation ring oriented with a fairly small tilting angle at the surface. When the concentration increased, the cation ring tended to lie flat at the surface, and the gauche defects of the butyl chain decreased due to the intermolecular chain-chain interactions and the consequent more ordered interfacial molecular arrangement. Additionally, the anti-symmetric stretching mode in the PPP and SPS spectra exhibited a peak shift, showing that there exists more than one kind of orientation or chemical environment for the butyl CH_3 group. These results may shed new light on understanding the surface behavior of water-miscible ionic liquids as well as the imidazolium based surfactants.

Key words: Sum frequency generation vibratinal spectroscopy, Ionic liquid, Aqueous solution, Interface, orientation

I. INTRODUCTION

Room temperature ionic liquids (RTILs) are organic salts composed entirely of ions and melt at temperature below 373 K. They can serve as "green" solvents because RTILs can be easily designed to be environmentally benign by choosing the suitable ion pairs from the unlimited numbers of combinations of cations and anions. Widespread usages have been found for the RTILs in both academic and industrial applications due to their unique characteristics: negligible vapor pressures [1], wide liquidus ranges [2], high conductivities [3], good thermal stabilities [4] and large electrochemical windows [5]. Some recent investigations have been focused on the 1-alkyl-3-methylimidazolium cation ([$C_n$mim]$^+$)-based RTILs, of which the cation consists of a hydrophobic tail and a hydrophilic head group. The latter makes the ILs water-miscible. Therefore this type of ILs can be mixed with water, another widely used "green" solvent, to form a binary system with potential applications in many areas including medical extraction [6], absorption cooling cycle [7], analytical chemistry [8], synthesis [9] and catalysis [10].

The presence of water in ILs can strongly influence the properties of ILs such as the heat capacity [11], density [12, 13], viscosity [14], electrical conductivity [15], and surface tension [16]. Additionally, some ILs in aqueous solutions exhibit surfactant-like behaviors due to the amphiphilic nature of the organic cation. By changing the alkyl chain length of the cation or the size of the anion, one could tune the hydrophobicity of the ILs and observe different aggregation behaviors of ILs in water [17]. It has also been found that the addition of even a small amount of ionic liquid can significantly affect the properties of aqueous solutions of surfactants [18−20] as short-alkyl-chain ionic liquids can be more than just a solvent but a co-surfactant [20], second surfactant [21], or even a single surfactant component [22−26]. Examples include [bmim][BF_4] (1-butyl-3-methylimidazolium tetrafluoroborate) and [bmim][CH_3SO_4] that were found to exhibit surfactant-like self-aggregations in aqueous solutions [22, 26].

[Bmim][BF_4] (see Fig.1 for the molecular structure) is a water-miscible ionic liquid that has been frequently

*Authors to whom correspondence should be addressed. E-mail: zhoulu@iccas.ac.cn, guoyuan@iccas.ac.cn, Tel.: +86-10-62571067, FAX: +86-10-62563167

 ©2013 Chinese Physical Society

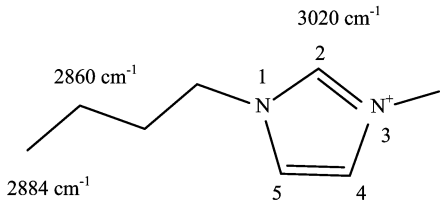

FIG. 1 Molecular structure of 1-butyl-3-methylimidazolium. The frequencies of the symmetric stretching modes of the butyl CH_3, butyl CH_2 and the stretching vibration of the imidazolium C(2)−H were also labeled accordingly.

studied. Both bulk [6, 27−30] and interfacial [22, 31−34] properties of its aqueous solution have been extensively investigated by various techniques. Kim and co-workers studied the air-liquid interface of the binary system of [bmim][BF_4]+water by both the surface tension and sum frequency generation (SFG) measurements [33, 34]. They suggested that at relatively low bulk concentrations of [bmim][BF_4], the liquid surface was covered by [bmim] cations, and when the bulk concentrations reached 0.02 mole fraction, the anions started to appear at the surface. The observed abnormal surface tension minimum around 0.016 mole fraction may be related to the adsorption of the anions at the surface. They also concluded that the methyl group of the butyl chain did not change too much with concentrations. Another SFG study of the [bmim][BF_4]+water binary system was carried out by Baldelli and co-worker [32]. They probed the orientations and structures of both the cation and water at the air/liquid interface. Their results suggested that the cation ring lied nearly parallel to the surface plane and the interactions between water and ionic liquid did not significantly influence the orientation of interfacial cations. Most of the RTIL concentrations studied by Kim and Baldelli were larger than 0.02 mole fraction (>1.1 mol/L). Apparently, there had been a lack of the studies on the [bmim][BF_4] aqueous solutions at low concentrations, which deserve more attentions because many imidazolium-based surfactants have very low critical micelle concentrations (mmol/L) [35].

In the present work, we used SFG to investigate the cation orientations and chain-chain interactions at the air/liquid interface of the [bmim][BF_4] aqueous solutions at a series of low bulk concentrations (0.004−1.1 mol/L). The reorientation of the imidazolium ring and the different chain-chain interactions were observed when the [bmim][BF_4] bulk concentration changed, revealing that the interfacial structures of the RTIL aqueous solutions are indeed a function of the bulk concentrations. It was also shown that the interactions between the water and RTIL molecules ought not to be overlooked for the low concentrations.

II. BASIC THEORY OF SFG

Sum frequency generation vibrational spectroscopy (SFG-VS) is a surface-specific nonlinear vibrational spectroscopic technique. The details of the SFG theory have been well described in previous studies [36, 37]. Generally, in a SFG-VS experiment, a visible beam $I_{\rm vis}$ at $\omega_{\rm vis}$ and a tunable infrared (IR) beam $I_{\rm IR}$ at $\omega_{\rm IR}$ overlap at the interface of the sample. By tuning the IR frequency and detecting the sum frequency ($\omega_{\rm SF}=\omega_{\rm vis}+\omega_{\rm IR}$) signal, we can obtain the vibrational spectra of the interfacial molecular species. The SFG signal intensity $I(\omega_{\rm SF})$ is given by

$$I(\omega_{\rm SF}) \propto |\chi_{\rm eff}|^2 I_{\rm vis}(\omega_{\rm vis}) I_{\rm IR}(\omega_{\rm IR}) \tag{1}$$

where $\chi_{\rm eff}$ is the effective second order susceptibility and can be expressed as

$$\chi_{\rm eff} \propto \chi_{\rm NR} + \sum_q \frac{A_q}{\omega_{\rm IR} - \omega_q + i\Gamma_q} \tag{2}$$

In Eq.(2), $\chi_{\rm NR}$ denotes the non-resonant term. A_q, ω_q and Γ_q represent the sum frequency strength factor tensor, resonant frequency and damping constant of the qth vibrational mode, respectively.

III. EXPERIMENTS

A. Sample preparation

Tetrafluoroborate salt of [bmim][BF_4], purity better than 99%, water content <350 ppm, chloride content <20 ppm, was purchased from Merck in Germany, and used without further purification. The liquid water was purified with a Millipore Simplicity 185 (18.2 MΩ·cm) from double distilled water.

B. SFG experiment

The experimental setup used in the present work has been described in detail previously [38]. Briefly, a 10-Hz and 23-ps SFG spectrometer laser system was purchased from EKSPLA. The visible wavelength was fixed at 532 nm and the full range of the IR tunability was 1000−4000 cm^{-1}. During the experiment, IR frequency was scanned with a 2-cm^{-1} increment and each point was averaged over 300 laser pulses. The energy of the visible pulse was set at 180 μJ and the energy of the IR pulse was less than 200 μJ. A co-propagate configuration was adopted. The incident angles of the visible and IR beams were 45° and 58° from the surface normal, respectively. A high-gain low-noise photomultiplier (Hamamatsu, PMT-R585) and a dual channel Boxcar average system (Stanford Research Systems) were integrated to serve as the signal detection system.

DOI:10.1063/1674-0068/26/05/569-575 ©2013 Chinese Physical Society

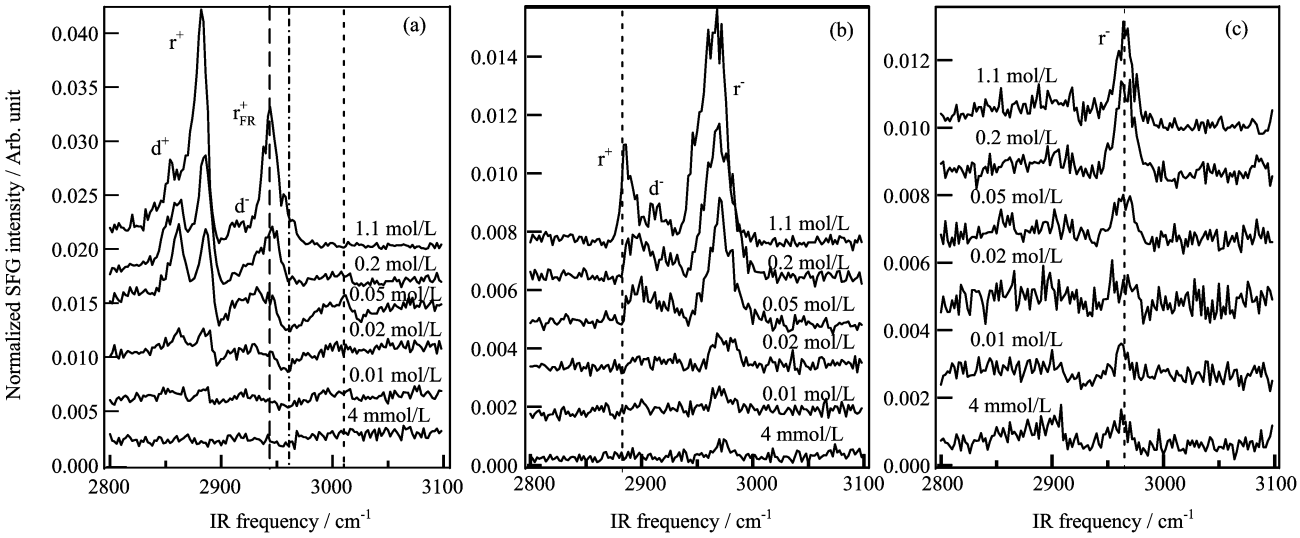

FIG. 2 SFG spectra of [bmim][BF$_4$] aqueous solution at different concentrations: 0.004, 0.01, 0.02, 0.05, 0.2, 1.1 mol/L with (a) SSP, (b) PPP, and (c) SPS polarization combinations. The spectra at different concentrations were offset for clarity.

The voltage of R585 was set at 1.3 kV for the measurement of IL aqueous solutions and 900 V for the measurement of the Z-cut quartz. The liquid sample was housed in a round Teflon beaker (with the diameter of 5 cm) for SFG measurements. The SFG spectra of three polarization combinations SSP, PPP, and SPS were carried out. Here SSP means the electric field vectors of the sum frequency signal beam, the incident visible and IR beam were S, S, and P, respectively (S represents that the electric field vector of the optical beam is perpendicular to the incident plane while P represents that the electric field vector is in the incident plane). The polarization combination terms of PPP and SPS were defined in a similar way. The measured spectra was first normalized by the energy of the incident laser beams, then normalized by the SFG signals from the Z-cut quartz (also normalized by the energy of the incident lasers), the details of the normalization procedure can be found in Refs.[38, 39]. All the measurements were carried out at controlled room temperature (22.0±0.5 °C) and humidity (40%).

IV. RESULTS AND DISCUSSION

Figure 2 shows the Z-cut-quartz normalized SFG spectra of the air/[bmim][BF$_4$] aqueous solution interface in the C−H stretching region for six different concentrations (0.004, 0.01, 0.02, 0.05, 0.2, 1.1 mol/L). The second highest concentration (0.2 mol/L) corresponds to the lowest concentration used in a previous study by Kim and co-workers [33]. In another previous study on the same system by Baldelli and co-workers [32], the RTIL concentrations were all higher than 0.01 mole fraction (1.1 mol/L) except one (2×10^{-4} mole fraction, close to 0.01 mol/L). Here we focused on the low concentrations due to a lack of the studies on the [bmim][BF$_4$] aqueous solutions at low concentrations.

Three different polarization combinations SSP, PPP, and SPS (Fig.2) were employed in this work. There were four apparent peaks around 2860, 2884, 2914, and 2945 cm^{-1} in SSP spectra. Peak assignments were based on the previous SFG reports on [bmim][BF$_4$] [33]. The peaks at 2860 and 2914 cm^{-1} were attributed to the CH$_2$ symmetric stretch mode (d$^+$) and CH$_2$ anti-symmetric stretch mode (d$^-$) of the butyl chain, respectively. The peaks at 2884 and 2945 cm^{-1} were assigned to the butyl CH$_3$ symmetric stretch mode (r$^+$) and Fermi resonance (r$^+_{\rm FR}$), respectively [33]. The peak at 2965 cm^{-1} in PPP and SPS spectra was assigned to CH$_3$ anti-symmetric stretch mode (r$^-$) of the butyl chain. The peak at 2884 and 2914 cm^{-1} in PPP spectra for high concentrations were also attributed to r$^+$ and d$^-$, respectively. As shown in Fig.2 the SSP and PPP spectra changed significantly as the bulk concentration increased. At 0.004 mol/L the SSP spectra showed no vibrational features for hydrocarbons but only a tail of the broad peak of the hydrogen bonded water. However, a small peak around 2965 cm^{-1} (r$^-$) began to rise in the PPP and SPS spectra at this concentration. This means even at very low concentrations (4 mmol/L) the cations are already adsorbed on the surface of the solution.

Many research groups choose to use a single polarization combination in the SFG studies, and the SSP polarization has been mostly used for the liquid interface. In some cases such as aqueous solutions, the SSP spectra show no clear C−H or N−H features in the region of 2800−3200 cm^{-1}, as shown in Fig.2(a) for the 4 mmol/L [bmim][BF$_4$] solution. But this does not necessarily mean there is no C−H or N−H containing species adsorbed to the surface because the SSP signals

DOI:10.1063/1674-0068/26/05/569-575 ©2013 Chinese Physical Society

of C−H or N−H may be buried in the broad peak of hydrogen bonded water. On the other hand, the SFG intensity of hydrogen bonded water in PPP or SPS spectra is much smaller than that in the SSP spectra [38, 40], giving a chance for the C−H or N−H vibrations to be observed in the PPP or SPS spectra. That is why some C−H features were observed in the PPP and SPS spectra instead of in the SSP spectra in the case of 4 mmol/L [bmim][BF_4] solution. This also proved the importance and necessity of polarization analysis in SFG spectra [36, 41, 42].

As mentioned above, at the very low [bmim][BF_4] concentration (4 mmol/L) the SSP spectrum showed few C−H features but only the tail of the hydrogen bonded water network. This is because the surface was still mostly occupied by water molecules at such a low concentration. When the concentration increased to 0.02 and 0.05 mol/L, the interference between the SFG signals of C−H and hydrogen bonded water was observed in SSP spectra because for these two concentrations the surface populations of the [bmim] cation and the water molecule were both fairly large and the SSP signals from the surface-bound organic cations and hydrogen-bonded water molecules were comparable. As a result of such interferences, the r^+_{FR} peak (broken line in Fig.2(a)) overlapped with the broad tail of hydrogen bond spectra and produced a valley around 2960 cm^{-1} (dashed line in Fig.2(a)) in the SSP spectra of 0.02 and 0.05 mol/L solutions. The valley, which was shifted away from the normal peak position of 2945 cm^{-1} for r^+_{FR}, was most likely due to the destructive interference between the r^+_{FR} and hydrogen bonded water peaks that have the opposite relative phases [43]. This also indicates that the peak positions do not necessarily coincide with the apparent peaks or valleys when interference effects occur [44]. At higher concentrations (0.2 and 1.1 mol/L), the surface was mostly covered by the [bmim] cations. So the SFG signals were dominated by vibrational features of the [bmim] cation, and consequently the interference effects were not obvious in these spectra.

To comprehensively understand the interference effects and intermolecular interactions between adsorbed species and interfacial water, it would require several assumptions, especially the relative vibrational phase between the two species. A systematic but qualitative discussion on this matter can be found in a previous SFG study on the mixed lipid-surfactant films by Walker and co-workers [43], therefore the detailed analysis of the interference effects will not be the focus of this work. In a short summary, the interference effects complicated the SFG spectra at several certain concentrations in the current work, and made it more difficult to obtain adequate fitting results when using Eq.(2) to fit the SSP spectra. Therefore only qualitative analysis will be discussed for the SSP spectra below.

When the concentration increased to 0.01 and 0.02 mol/L, the d^+ and r^+ peaks started to rise with the SSP polarization. To understand the change of the relative intensities of the SSP peaks for all concentrations, the local conformations of the CH_2 hydrocarbon backbone should be considered. The d^+ peak usually is considered as a measure of the order/disorder degree for the alkyl chains [45−47]. A larger d^+ intensity in SFG spectra indicates that the alkyl chains are poorly ordered with a high degree of gauche defect, and a smaller d^+ peak can be used as the evidence of a well ordered monolayer with all-*trans* hydrocarbon chains. In Fig.2(a), the relatively large d^+ intensities in SSP spectra for the 0.02 and 0.05 mol/L solutions led to the conclusion that the adsorbed cations at the surface were disorganized with a high degree of the gauche defect for the butyl chain at low RTIL concentrations. When the concentration increased, the d^+ peak gradually merged into the shoulder of the strong r^+ peak. For the case of pure [bmim][BF_4], the d^+ peak were barely seen from the SFG spectra [33, 34]. This may suggest that at low concentrations the surface-adsorbed cations were in small amounts and loosely packed, so the cations were poorly organized. When the concentration increased, more cations were adsorbed to the surface and became more densely packed. Due to the chain-chain interactions, less space was available for the chain reorientations, and the *trans*-gauche bond isomerization became restricted [47].

Another interesting feature of SSP spectra is that for the 0.01, 0.02, 0.05, and 0.2 mol/L solutions, there was a small peak around 3010 cm^{-1} assigned to the C−H stretch at the C(2) carbon of the cation ring [48, 49]. This peak has never been observed for the aqueous solution at higher (>1.1 mol/L) concentrations or pure [bmim][BF_4]. It can be interpreted that at high concentrations or for the pure [bmim][BF_4], the cation ring lies flat at the surface, so the C(2)−H bond is parallel to the surface and can not generate detectable SFG signals. In the present study, at low concentrations, the C(2)−H stretch features appeared above the noise level in the SSP spectra, suggesting that the cation ring adopted a fairly small tilt angle instead of lying completely flat at surface at low bulk [bmim][BF_4] concentrations. When the concentration increased to 1.1 mol/L, this peak disappeared, meaning that the cation ring became lying more parallel to the surface at this high concentration, in agreement with the previous SFG study [32]. The variation of the C(2)−H stretch peak intensities indicated there existed a reorientation process of the cation ring when the RTIL concentration increase. As mentioned above, the interference between the SFG signals of the C−H stretch and the hydrogen bonded water made it difficult to adequately fit the SSP spectra, so only qualitative discussions are presented here.

With a closer examination of the SSP spectra of d^+ and C(2)−H stretch region, we found another interesting spectral feature that the intensity of d^+ and C(2)−H stretch shared the same trend. Both of the peaks were small in the 0.01 mol/L solution and rose

DOI:10.1063/1674-0068/26/05/569-575 ©2013 Chinese Physical Society

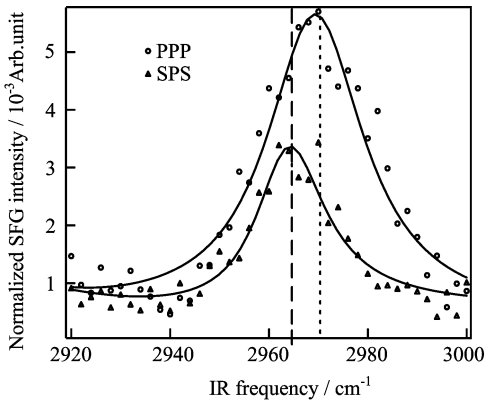

FIG. 3 The expanded portion of 0.2 mol/L PPP and 0.2 mol/L SPS spectra in r$^-$ region. The solid lines are the fitting results. The broken and dashed lines are guide for the eye of peak positions of SPS and PPP, respectively.

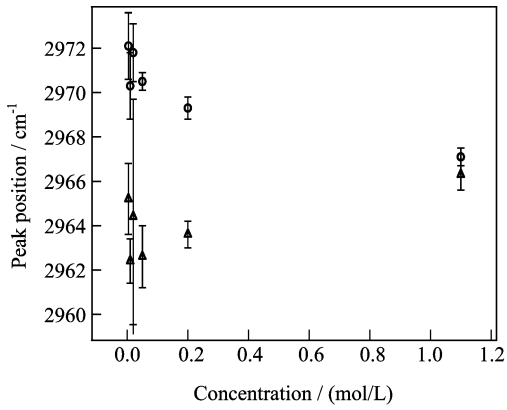

FIG. 4 The peak positions of the CH$_3$ (butyl chain) antisymmetric stretch mode (r$^-$) for PPP (circle) and SPS (triangle) polarizations obtained by fitting the spectra using Eq.(2).

up when the concentration increased. When the concentration reached 0.05 mol/L, both peaks approached their maximum SFG intensities. As the concentration continued to increase to the value of 1.1 mol/L, both peaks began to decrease again, the d$^+$ peak dissolved into the shoulder of the r$^+$ peak while the C(2)−H stretch disappeared. This suggested that the reconstruction of the butyl chain packing and the reorientation of the imidazolium ring are related to each other in some way. Although how exactly the two processes are related to each other needs further experimental and theoretical studies, the observed reconstructions of the surface-bound organic cation arrangements indicated the changing interactions between the adsorbed species and the interfacial water molecules and also between the adsorbed species themselves. These observations can also be used to explain the surface properties of RTIL solutions such as viscosity and surface tensions at different conditions.

The complexity of the surface of the RTIL solutions can be further evidenced by a close comparison of PPP and SPS spectra in the r$^-$ region where a disparity of r$^-$ peak position between PPP and SPS spectra was revealed. Figure 3 shows the expanded PPP and SPS spectra in the r$^-$ vibrational region. Only the spectra of the 0.2 mol/L solution were shown in Fig.3 since different concentrations exhibited similar results (see supplementary material). As shown in Fig.3, the r$^-$ peak position with the SPS polarizaiton was red-shifted compared with the corresponding PPP peak. By fitting the SFG spectra using Eq.(2) we obtained the r$^-$ peak positons for both polarizations. The resulting PPP and SPS peak positions from spectral fitting for different [bmim][BF$_4$] concentrations were plotted in Fig.4. Other fitting parameters are listed in the Table S1 in the supplementary material. We can see that the peak positions of r$^-$ peak with the PPP polarization were around 2970 cm^{-1} and shifted to around 2963 cm^{-1} for SPS polarization. The only exception was the concentration of 1.1 mol/L, of which the r$^-$ peak position in the PPP spectra was very close to that in the SPS spectra. The reason for the seemingly red-shift of r$^-$ peak in the PPP spectra at 1.1 mol/L was that the PPP intensity of r$^+_{\rm FR}$ mode became stronger at high concentrations and the rising $r^+_{\rm FR}$ peak merged into the shoulder of the r$^-$ peak. So when using a single r$^-$ peak to fit the PPP spectra at 1.1 mol/L, the peak position will shift to the red side compared with the actual r$^-$ position. This can be further supported by the SFG measurement on the pure [bmim][BF$_4$], where the r$^-$ peak positions in the PPP and SPS spectra also seemed to be close to each other (see Fig.S2(a) in the supplementary material) for the same experimental configuration as used in the present study (visible 45°, IR 58°). To separate the overlapping r$^-$ and r$^+_{\rm FR}$ peaks in the PPP spectra for the pure [bmim][BF$_4$], we switched to another experimental configuration (visible incident angle 55°, IR incident angle 41°), with which the intensity of r$^+_{\rm FR}$ in PPP spectra became much smaller and did not disturb the r$^-$ peak anymore. It was observed at this new experimental configuration that the r$^-$ peak positions in the PPP and SPS spectra split just as the case of the low concentrations (see Fig.S2(b) in the supplementary material). A more systematic investigation on the surface structure of the RTIL surface by comparing different SFG spectra from a variety of the experimental configurations (laser incident angles) is currently undergoing, and we observed the spectral splitting in the r$^-$ vibrational region at all the RTIL samples.

This observed spectral shift in the r$^-$ region for the [bmim][BF$_4$] aqueous solutions could not arise from the possible N−CH$_3$ symmetric stretch mode at 2975 cm^{-1}, because no clear spectral features appeared around 2975 cm^{-1} in the SSP spectra. According to the polarization selection rule for the CH$_3$ symmetric stretch mode, the SSP intensity should always be many times

DOI:10.1063/1674-0068/26/05/569-575 ©2013 Chinese Physical Society

of that of the PPP and SPS [42], which was not the case observed in this work for the 2960−2970 cm^{-1} region. Therefore the N−CH_3 group could not be the reason of the peak shift as shown in Fig.3 and Fig.4. Ruling out the possible contributions of the N−CH_3 group, we conclude that the split peaks in the 2960−2970 cm^{-1} region in the PPP and SPS spectra shall both originate from the butyl CH_3 r^- mode. The reason for the spectral splitting is that there exist more than one kind of butyl CH_3 groups which have slightly different chemical environments and vibrational frequencies, possibly due to the CH_3 (butyl chain) with different orientations [51] or located in the different interfacial layers. This is also in agreement with the relatively disorganized [bmim] surface structures at low concentrations observed by the d^+ spectra mentioned earlier in this work.

V. CONCLUSION

We reported the polarization-dependent sum frequency generation vibrational spectroscopy study of the air/[bmim][BF_4] aqueous solution interfaces at low concentrations. The SFG spectra showed the organic cations were poorly ordered at the surface with the butyl chain exhibiting a high degree of gauche defect at low concentrations. When the [bmim][BF_4] concentration increased, more cations adsorbed to the surface and became well-ordered at the surface. As a result the *gauche* defect decreased due to the chain-chain interaction at higher concentrations. There also existed a reorientation process of the cation ring when the concentration increased as observed by the change of C(2)−H stretching peak intensities. In addition, the PPP and SPS spectra exhibited a peak shift for the butyl CH_3 antisymetric stretching mode (r^-) between the two polarizations, indicating that there existed more than one kind of butyl CH_3 groups due to the different molecular orientations or chemical environments. These results may be useful for understanding the surface behaviors of water miscible ionic liquids and imidazolium based surfactants. The reorientation of the butyl chain and the cation ring, as well as the existence of different types of CH_3 (butyl chain), indicated that the surface structure of [bmim][BF_4] aqueous solutions at low concentrations is more complicated than expected. More quantitative experiment and theoretical studies are needed.

VI. ACKNOWLEDGMENTS

This work was supported by the National Natural Science Foundation of China (No.21073199, No.91027042, and No.21227802) and the Ministry of Science and Technology of China (No.2013CB834504).

Supplementary material: The r^- region in the SPS and PPP spectra of different concentrations and experimental configurations can be found in the supplementary material.

[1] J. Esperanca, J. N. C. Lopes, M. Tariq, L. Santos, J. W. Magee, and L. P. N. Rebelo, J. Chem. Eng. Data. **55**, 3 (2010).
[2] J. D. Holbrey and R. D. Rogers, *Ionic Liquids in Synthesis*, 2nd Ed., Weinheim: Wiley-VCH, (2008).
[3] H. Ohno, *Electrochemical Aspects of Ionic Liquids*, 2nd Ed., New Jersey: Wiley Hoboken, (2011).
[4] C. P. Fredlake, J. M. Crosthwaite, D. G. Hert, S. Aki, and J. F. Brennecke, J. Chem. Eng. Data. **49**, 954 (2004).
[5] P. A. Z. Suarez, V. M. Selbach, J. E. L. Dullius, S. Einloft, C. M. S. Piatnicki, D. S. Azambuja, R. F. deSouza, and J. Dupont, Electrochim. Acta **42**, 2533 (1997).
[6] F. Y. Du, X. H. Mao, and G. K. Li, J. Chromatogr. A **1140**, 56 (2007).
[7] A. Yokozeki and M. B. Shiflett, Ind. Eng. Chem. Res. **49**, 9496 (2010).
[8] R. J. Soukup-Hein, M. M. Warnke, and D. W. Armstrong, Annu. Rev. Anal. Chem. **2**, 145 (2009).
[9] X. H. Zhao, Y. Y. Gu, J. Li, H. M. Ding, and Y. K. Shan, Catal. Commun. **9**, 2179 (2008).
[10] C. Chiappe, L. Neri, and D. Pieraccini, Tetrahedron Lett. **47**, 5089 (2006).
[11] L. P. N. Rebelo, V. Najdanovic-Visak, Z. P. Visak, M. N. da Ponte, J. Szydlowski, C. A. Cerdeirina, J. Troncoso, L. Romani, J. Esperanca, H. J. R. Guedes, and H. C. de Sousa, Green Chem. **6**, 369 (2004).
[12] J. Jacquemin, P. Husson, A. A. H. Padua, and V. Majer, Green Chem. **8**, 172 (2006).
[13] H. Rodriguez and J. F. Brennecke, J. Chem. Eng. Data **51**, 2145 (2006).
[14] K. R. Seddon, A. Stark, and M. J. Torres, Pure Appl. Chem. **72**, 2275 (2000).
[15] J. A. Widegren, E. M. Saurer, K. N. Marsh, and J. W. Magee, J. Chem. Thermodyn. **37**, 569 (2005).
[16] M. Tariq, M. G. Freire, B. Saramago, J. A. P. Coutinho, J. N. Canongia Lopes, and L. P. N. Rebelo, Chem. Soc. Rev. **41**, 829 (2012).
[17] M. Blesic, M. H. Marques, N. V. Plechkova, K. R. Seddon, L. P. N. Rebelo, and A. Lopes, Green Chem. **9**, 481 (2007).
[18] A. Beyaz, W. S. Oh, and V. P. Reddy, Colloids Surf. B **36**, 71 (2004).
[19] K. Behera and S. Pandey, J. Phys. Chem. B **111**, 13307 (2007).
[20] Y. Z. Shang, T. F. Wang, X. Han, C. J. Peng, and H. L. Liu, Ind. Eng. Chem. Res. **49**, 8852 (2010).
[21] F. Comelles, I. Ribosa, J. J. Gonzalez, and M. T. Garcia, Langmuir **28**, 14522 (2012).
[22] J. Bowers, C. P. Butts, P. J. Martin, M. C. Vergara-Gutierrez, and R. K. Heenan, Langmuir **20**, 2191 (2004).
[23] Z. Miskolczy, K. Sebok-Nagy, L. Biczok, and S. Gokturk, Chem. Phys. Lett. **400**, 296 (2004).
[24] J. J. Wang, H. Y. Wang, S. L. Zhang, H. H. Zhang, and Y. Zhao, J. Phys. Chem. B **111**, 6181 (2007).

DOI:10.1063/1674-0068/26/05/569-575 ©2013 Chinese Physical Society

[25] J. Luczak, J. Hupka, J. Thoming, and C. Jungnickel, Colloids Surf. A **329**, 125 (2008).
[26] A. Modaressi, H. Sifaoui, M. Mielcarz, U. Domanska, and M. Rogalski, Colloids Surf. A **302**, 181 (2007).
[27] M. Moreno, F. Castiglione, A. Mele, C. Pasqui, and G. Raos, J. Phys. Chem. B **112**, 7826 (2008).
[28] Y. Jeon, J. Sung, C. Seo, H. Lim, H. Cheong, M. Kang, B. Moon, Y. Ouchi, and D. Kim, J. Phys. Chem. B **112**, 4735 (2008).
[29] I. B. Malham, P. Letellier, and M. Turmine, J. Phys. Chem. B **110**, 14212 (2006).
[30] D. G. Archer, J. A. Widegren, D. R. Kirklin, and J. W. Magee, J. Chem. Eng. Data **50**, 1484 (2005).
[31] J. W. Russo and M. M. Hoffmann, J. Chem. Eng. Data **55**, 5900 (2010).
[32] S. Rivera-Rubero and S. Baldelli, J. Phys. Chem. B **110**, 15499 (2006).
[33] J. Sung, Y. Jeon, D. Kim, T. Iwahashi, T. Iimori, K. Seki, and Y. Ouchi, Chem. Phys. Lett. **406**, 495 (2005).
[34] J. Sung, Y. Jeon, D. Kim, T. Iwahashi, K. Seki, T. Iimori, and Y. Ouchi, Colloids Surf. A **284**, 84 (2006).
[35] N. A. Smirnova, A. A. Vanin, E. A. Safonova, I. B. Pukinsky, Y. A. Anufrikov, and A. L. Makarov, J. Colloid Interf. Sci. **336**, 793 (2009).
[36] X. Zhuang, P. B. Miranda, D. Kim, and Y. R. Shen, Phys. Rev. B **59**, 12632 (1999).
[37] H. F. Wang, W. Gan, R. Lu, Y. Rao, and B. H. Wu, Int. Rev. Phys. Chem. **24**, 191 (2005).
[38] W. Gan, D. Wu, Z. Zhang, R. R. Feng, and H. F. Wang, J. Chem. Phys. **124**, 114705 (2006).
[39] X. Wei, S. C. Hong, X. W. Zhuang, T. Goto, and Y. R. Shen, Phys. Rev. E **62**, 5160 (2000).
[40] X. Wei and Y. R. Shen, Phys. Rev. Lett. **86**, 4799 (2001).
[41] R. Lu, W. Gan, B. H. Wu, H. Chen, and H. F. Wang, J. Phys. Chem. B **108**, 7297 (2004).
[42] R. Lu, W. Gan, B. H. Wu, Z. Zhang, Y. Guo, and H. F. Wang, J. Phys. Chem. B **109**, 14118 (2005).
[43] S. Z. Can, C. F. Chang, and R. A. Walker, Biochim. Biophys. Acta **1778**, 2368 (2008).
[44] D. Wu, G. H. Deng, Y. Guo, and H. F. Wang, J. Phys. Chem. A **113**, 6058 (2009).
[45] M. J. Hostetler, J. J. Stokes, and R. W. Murray, Langmuir **12**, 3604 (1996).
[46] J. C. Conboy, M. C. Messmer, and G. L. Richmond, J. Phys. Chem. B **101**, 6724 (1997).
[47] T. Iimori, T. Iwahashi, K. Kanai, K. Seki, J. Sung, D. Kim, H. O. Hamaguchi, and Y. Ouchi, J. Phys. Chem. B **111**, 4860 (2007).
[48] D. A. Carter and J. E. Pemberton, J. Raman. Spectrosc. **28**, 939 (1997).
[49] C. Romero and S. Baldelli, J. Phys. Chem. B **110**, 6213 (2006).
[50] L. Velarde, X. Y. Zhang, Z. Lu, A. G. Joly, Z. M. Wang, and H. F. Wang, J. Chem. Phys. **135**, 241102 (2011).

DOI:10.1063/1674-0068/26/05/569-575 ©2013 Chinese Physical Society